ASIAN JOURNAL OF PHARMACEUTICAL AND CLINICAL RESEARCH

INNOVARE ACADEMIC SCIENCES
Knowledge to Innovation

Vol 18, Issue 9, 2025

Online - 2455-3891
Print - 0974-2441

Research Article

MIMOSA PUDICA-LOADED NANOEMUGEL: A PROMISING TOPICAL SYSTEM FOR SKIN CANCER MANAGEMENT

VAISHALI GAIKWAD[1]*, RAVINDRA LAWARE[2], NITIN MOHIRE[3], SOMNATH BHINGE[4]

[1]Department of Pharmaceutical Sciences, Bhagwant University, Ajmer, Rajasthan, India. [2]Department of Pharmaceutics, College of Pharmaceutical Sciences, Pravara Institute of Medical Sciences (Deemed to be University), Loni, Maharashtra, India. [3]Department of Pharmacology, Shivajirao S. Jondhle College of Pharmacy, Thane, Maharashtra, India. [4]Department of Pharmaceutical Chemistry, Krishna Vishwa Vidyapeeth (Deemed to be University), Krishna Institute of Pharmacy, Karad, Maharashtra, India.
***Corresponding author: Vaishali Gaikwad; Email: gitamohire123@gmail.com**

Received: 13 June 2025, Revised and Accepted: 25 July 2025

ABSTRACT

Objectives: The skin, being the body's largest organ, functions as a vital protective barrier but is highly vulnerable to environmental challenges, including chemical mutagens and carcinogens encountered daily. This study focuses on the development and characterization of *Mimosa pudica*-loaded PLAROsomes nanoemugel for enhanced therapeutic efficacy against skin cancer.

Methods: A nanoemugel containing *M. pudica* extract (2.5% w/w) and Carbopol Ultrez 10 NF (2.5% w/w) using a modified formulation approach. The objective was to enhance the solubility, permeation, and therapeutic efficacy of *M. pudica* for treating skin cancer. The formulation incorporated rose oil and oleic acid, combined with Tween 20 and propylene glycol as a Smix system. Comprehensive evaluation of the nanoemugel was conducted, including *in vitro* drug release, viscosity assessment, thermal and morphological analyses (scanning electron microscopy and transmission electron microscopy [TEM]), globule size distribution, zeta potential measurement, *in vitro* cytotoxicity through the MTT assay.

Results: The thermal analysis of the formulation revealed its thermal stability and highlighted potential interactions between the *M. pudica* extract and the PLARosomal matrix. The nanoemugel demonstrated a globule size of 122.9 nm, with TEM analysis confirming particle agglomeration and circular morphology, measuring 82.3±12 nm. A sustained drug release profile was observed, with cumulative release reaching 68.25% over 48 h. Stability studies confirmed the formulation's robustness under storage conditions. *In vitro* cytotoxicity assays on cancer cells showed enhanced efficacy, with a cell viability percentage of 50.21% at a concentration of 100 µg mL^{-1}.

Conclusion: These findings indicate that *M. pudica*-loaded PLAROsomes nanoemugel is a promising candidate for targeted topical therapy in skin cancer treatment.

Keywords: *Mimosa pudica*, Skin cancer, Cytotoxicity, Nanoemugel.

 DOI: http://dx.doi.org/10.22159/ajpcr.2025v18i9.55567. Journal homepage: https://innovareacademics.in/journals/index.php/ajpcr

INTRODUCTION

The skin, as the body's largest organ, serves as a critical barrier but remains susceptible to various environmental insults, including chemical mutagens and carcinogens encountered in daily life [1]. Cancer is one of the leading causes of morbidity and mortality globally, with its prevalence increasing due to environmental and lifestyle changes [2]. Skin cancer, in particular, has emerged as a significant public health concern, driven by factors such as heightened exposure to ultraviolet radiation and environmental pollutants [3]. In India, the prevalence of skin neoplasms constitutes approximately 2–3% of all reported cancers, while globally, non-melanoma skin cancer accounts for more cases annually than all other cancer types combined [4,5].

Topical drug delivery systems have gained substantial attention for their non-invasive approach, which offers localized treatment and improved patient compliance compared to oral or parenteral methods [6]. However, the outermost layer of the skin, the stratum corneum, presents a formidable barrier to drug permeation, necessitating innovative strategies to enhance drug delivery [7]. Among these, nanoparticulate drug delivery systems have shown great promise, offering benefits such as enhanced penetration, controlled release, and protection of active compounds from degradation [8,9].

Nanoemulsion-based gels are a cutting-edge advancement in this field, combining the advantages of nanoemulsions and gels to optimize drug delivery. These formulations feature nanosized droplets dispersed within a gel matrix, imparting unique properties such as improved absorption, stability, and controlled drug release [10]. The versatility of Nanobiogels extends to various applications, including cancer therapy and skincare, due to their ability to deliver active agents effectively to deeper layers of the skin [11]. This study delves into the potential of NBGs as advanced carriers for topical drug delivery, emphasizing their capacity to address challenges in solubility, bioavailability, and site-specific targeting.

Mimosa pudica, a perennial herb commonly known as the "touch-me-not" plant, has garnered significant attention due to its medicinal properties, particularly in wound healing, anti-inflammatory, and antimicrobial activities [12,13]. The phytochemical constituents of *M. pudica*, including alkaloids, flavonoids, tannins, and terpenoids, contribute to its wide-ranging pharmacological effects [14]. Among these, its rich flavonoid content has been linked to potential antitumor properties, making it an intriguing candidate for cancer therapy [15]. Flavonoids such as quercetin and rutin in *M. pudica* are known to exert antioxidant effects, scavenging free radicals and reducing oxidative stress, which are critical in the pathogenesis of various diseases, including cancer [16,17].

Despite its promising therapeutic potential, challenges remain in harnessing *M. pudica*'s bioactive compounds for clinical applications due to issues such as poor solubility, stability, and bioavailability.

Conventional formulations often exhibit limited efficacy, prompting the need for novel drug delivery systems to optimize the delivery of its active components [18]. Nanoemulsion-based systems have emerged as a cutting-edge approach to overcome these barriers, offering enhanced solubility, targeted delivery, and controlled release [19]. Recent advancements have explored nanoemulsions and microemulsions for encapsulating *M. pudica* extracts, with researchers reporting improved bioavailability and efficacy against cancer cell lines [20].

For instance, Das *et al*. formulated a nanoemulsion of *M. pudica* extract using response surface methodology, achieving a drug release rate of over 85% within 12 h, coupled with significant cytotoxic activity against human melanoma cells [21]. Similarly, Shah *et al*. developed a nanoparticle-based gel incorporating *M. pudica*, which exhibited enhanced permeation across the skin and prolonged action, addressing the limitations of conventional topical formulations [22]. Despite these advancements, many studies have reported incomplete drug release profiles or suboptimal permeation rates, highlighting the need for further exploration and optimization of *M. pudica*-based drug delivery systems.

The present study builds on this groundwork, focusing on the development of an innovative nanoemulsion-based gel system for *M. pudica*. By leveraging advanced formulation techniques, this research aims to address the challenges of solubility, stability, and drug delivery, thereby unlocking its full therapeutic potential for topical applications.

The present study aims to formulate a nanoemulsion-based gel incorporating *M. pudica* extract to enhance its solubility and skin permeation, reduce potential side effects, and ultimately amplify its therapeutic efficacy against skin cancer cells, thereby maximizing its anticancer potential.

METHODS

Materials

Liquid paraffin, alkyl (2-methyl) resorcinol, lecithin (soya), and other high-performance liquid chromatography (HPLC) and analytical-grade solvents and chemicals were provided by LOBA Chem. Industries, Mumbai, Maharashtra. In addition, LOBA Chemie, Mumbai, supplied propylene glycol, oleic acid, propyl paraben, lactic acid (98%), phosphotungstic acid, and sodium hydroxide. Rose oil was sourced from Research Laboratory Fine Chem, Mumbai, and acetone was obtained from Merck Life Sciences Pvt. Ltd. Lubrizol Advanced Material India Pvt. Ltd., Gujarat, kindly provided Carbopol Ultrez 10 NF as a gift sample, and Tween 20 was received as a courtesy from Intas Pharmaceuticals Limited, Gujarat. The B16F10 cell line (mouse skin melanoma) were acquired from the National Centre for Cell Science (NCCS), Pune, Maharashtra. All chemicals, solvents, and reagents used throughout the study were of HPLC and analytical-grade standards.

Collection, authentication and extraction of *M. pudica*

The collection process of *M. pudica* material was carried out from a local herb garden, during the peak flowering season to ensure optimal phytochemical yield. The plant's identity was confirmed and verified, with a voucher specimen (Ref.: SE/AC/2023/65) deposited in the herbarium for future reference. Fresh aerial parts, including stems, leaves, and flowers, were harvested, cleaned thoroughly to cleanse of any debris or dirt, and then air-dried in the shade at room temperature to preserve the bioactive compounds. After being dried, the plant parts was ground into a fine powder with the help of a mechanical grinder. The grinded powder was subjected to extraction using ethanol, following a Soxhlet extraction method. Following this, the plant extract underwent concentration under reduced pressure with the aid of a rotary evaporator. Finally, the crude extract was kept in an airtight glass container at 26±3°C for future analysis.

Preparation and lyophilization of *M. pudica*-loaded PLAROsomes

For the development of *M. pudica*-loaded PLAROsomes formulation, thin-film hydration method [23,24] was employed as per the procedure mentioned under our work Gaikwad *et al*. [25]. The lyophilization was employed for the *M. pudica*-loaded PLAROsomes as per Gaikwad *et al*., in 2025. Following an overnight pre-freezing maintained at −55±5°C, the initial drying was continued using a vacuum freeze-dryer [26].

Formulation of *M. pudica* PLAROsomes nanoemulsion-based gel

The development of nanoemulsion involved selecting oils, surfactants, and co-surfactants based on prior research [27]. Initially, rose oil (2.14%) and oleic acid (10.71%) were combined in specified concentrations and stirred for 5 min on a magnetic stirrer (Stage 1). Prepared *M. pudica*-loaded PLARosomal formulation (2.5%) was then dissolved in this oil phase mixture with continuous stirring for 30 min (Stage 2), followed by the addition of lactic acid (0.95%) (Stage 3). Smix, comprising Tween 20 (19.28%) and propylene glycol (19.28%) in a 1:1 ratio as determined in a previous study [28], was prepared and incorporated into the oil phase as the organic phase (Stage 4 and Stage 5). The aqueous phase was prepared separately by hydrating Carbopol Ultrez 10 NF (2.5%) polymer in water containing traces of lactic acid (Stage 6). The organic phase was then gradually added to the aqueous phase under magnetic stirring (Stage 7). The resulting formulation was allowed to equilibrate overnight, and the pH was adjusted to 5.2 using traces of sodium hydroxide solution (18%) and methyl paraben (0.03%) as a preservative. Purified water was added to make the total (Table 1).

Characterization of *M. pudica*-loaded PLAROsomes nanoemugel

Physical appearance, viscosity, and pH analysis

The consistency, clarity, and uniformity of the *M. pudica*-loaded PLAROsomes Nanoemugel were evaluated through visual observation. The viscosity of the formulations was determined using a Brookfield viscometer equipped with spindle C75, operating at 100 rpm under controlled conditions of 25±2°C. The pH measurement of the nanoemugel was conducted using a digital pH meter (Hanna Instruments), which was calibrated beforehand with standard buffer solutions of pH 4 and pH 9. For pH analysis, approximately 1 g of the Nanoemulgel was dissolved in 100 mL of double-distilled water, and the solution's pH was recorded.

Spreadability studies

The spreadability of the *M. pudica*-loaded PLAROsomes nanoemugel was assessed by placing approximately 2 g of the formulation on a ground glass slide. This slide was then positioned beneath a second glass slide equipped with a hook, as described previously [29]. A predefined weight was attached to the hook and utilized for measurement through a pulley system. The time required for the slides to move apart through the nanoemugel under the applied load was recorded in seconds. The spreadability (*S*) was determined using the following equation:

$$S = ML/T \quad (1)$$

Where, M represents the weight applied to the pan, L is the distance from the hook to the centre of the pan, and T denotes the duration of the slide transition [30].

Table 1: Composition of *M. pudica*-loaded PLAROsomes nanoemugel

Composition (%w/w)	*M. pudica*-loaded PLAROsomes nanoemugel
M. pudica-loaded PLAROsomes	2.5
Oleic acid	10.71
Rose oil	2.14
Tween 20	19.28
Propylene glycol	19.28
Carbopolultrez 1	2.5
Lactic acid	0.95
Methyl paraben	0.03
Sodium hydroxide solution (18%)	q.s
Purified water (qs)	100

M. pudica: *Mimosa pudica*

Fourier-transform infrared spectroscopy (FTIR) analysis

The functional groups of *M. pudica* extract, *M. pudica*-loaded PLAROsomes nanoemugel, and their interactions with excipients were analyzed using FTIR spectroscopy over a range of 300–4200 cm^{-1}. Samples were placed on a designated holder and evaluated using a Bruker Alpha II FTIR spectrophotometer (Japan).

Differential scanning calorimetry (DSC)

The thermal behavior of *M. pudica*-Loaded PLAROsomes nanoemugel was analyzed using a Mettler Toledo DSC system (Star SW10). The samples were heated at a controlled rate of 20°C/min across a temperature range of 40°C–340°C under a constant nitrogen flow rate of 100 mL min^{-1}. Transition temperatures were identified by examining the minimum points of endothermic peaks observed in the DSC thermograms.

Thermo gravimetric analysis

Thermogravimetric analysis (TGA) was performed using a TGA 400 instrument (Perkin Elmer, USA). A sample of *M. pudica*-loaded PLAROsomes weighing 38.510 mg was subjected to heating at a constant rate of 10°C/min over a temperature range of 0°C–350°C. Nitrogen gas, flowing at a rate of 18 mL/min, was used as the protective atmosphere during the analysis [31].

Size distribution and globule size

The globule size and size distribution of *M. pudica*-Loaded PLAROsomes nanoemugel were evaluated using dynamic light scattering with a particle size/zeta potential analyzer (HORIBA Scientific SZ 100, Japan). The sample was diluted 1:100 with deionized water before analysis. The size measurement was performed for a duration of 100 s at a detection angle of 90° [32].

Zeta potential

The zeta potential of *M. pudica*-loaded PLAROsomes nanoemugel was measured using the HORIBA Scientific SZ-100 [32]. The sample was diluted 1:100 with deionized water before analysis. It was then placed into a transparent disposable zeta cell, where the measurement was conducted over 60 s.

Transmission electron microscopy (TEM)

The surface morphology of *M. pudica*-loaded PLAROsomes nanoemugel was analyzed using TEM (JEM-2100F, JEOL Ltd) at a voltage of 200 kV. The sample was placed on a carbon-coated copper grid and stained with a 1% (w/v) phosphotungstic acid solution. The air-dried sample was then examined under high-resolution-TEM [33].

% Drug release

The release studies were conducted with a buffer solution at pH 7.4 in a beaker containing 100 mL of solution. The prepared medium was carefully heated to a temperature of 38±3°C in a beaker, which was positioned on a magnetic stirrer to maintain consistent stirring and ensure even heating. For the experiment, a Sigma Aldrich dialysis bag having MWCO 12,000 Da was utilized, allowing for controlled diffusion of molecules during the study. *M. pudica*-loaded PLAROsomes nanoemugel dispersion after being added to the dialysis bag, the mixture was suspended in the prepared medium. Samples (5 mL) were extracted and filtered through a Whatman filter at various time points. In addition, the media were replenished to maintain the exact volume using prepared buffer solution. Finally, the collected aliquots and the polyphenol content were estimated utilizing the Folin–Ciocalteu assay over a study period of 24 h [34-36]. The drug release kinetic profiles were evaluated with mathematical models namely Zero order kinetics, First order kinetics, Higuchi, and Korshmayer Peppas. The equations corresponding to mathematical models were considered per the standard protocol given in Bhinge *et al*., 2024 [32].

***In vitro* anticancer activity**

MTT assay (PC-3 and B16F10 cells)

The *in vitro* anticancer activity of *M. pudica*-loaded PLAROsomes nanoemugel was evaluated against B16F10 (Mouse Skin Melanoma Cell Line). The cell lines were outsourced from the NCCS, Pune, and maintained in Ham's F12K medium supplemented with 10% fetal bovine serum. Cells were incubated at strength of 1×10^2 cells/mL under conditions of a humidified atmosphere of 5% carbon dioxide (CO_2) at 37°C.

For the MTT assay, cells were initially seeded at a strength of 10^2 cells/well in 70 µL culture medium in 96-well plates [37-39]. Following a 24-h incubation, 100 µL of varying concentrations of *M. pudica*-loaded PLAROsomes nanoemugel (10–100 µg mL^{-1}) was added to the labeled wells. Control wells received 0.2% dimethyl sulfoxide (DMSO) solution in phosphate-buffered saline (PBS) to assess baseline cell viability. All experiments were conducted in triplicate. After 24 h of incubation in a CO_2 incubator, the medium was gently discarded, and 20 µL of MTT reagent having the strength of 5 $mgmL^{-1}$ in PBS solution was introduced into each well. Cells were incubated for an additional 4 h to allow for formazan crystal formation, which was observed under a microscope [40]. The resulting crystals were made soluble by adding 200 µL of DMSO solution to each labeled well, followed by a 10-min incubation at 37±3°C, shielded from light with aluminum foil. The absorbance of each labeled sample well was noted at 570 nm using a Benesphera E21ELISA microplate reader. The results provided a quantitative assessment of cell viability, demonstrating the enhanced anticancer activity of *M. pudica*-loaded PLAROsomes Nanoemugel compared to control treatments.

Statistical analysis

The present study for the optimization of nano-emulsion gel was determined by applying 2 –way analysis of Variance with Bonferroni's multiplying comparison test and accomplished using GraphPad Prism 10.2 software. The findings were verified as statistically significant with a p-value below 0.05.

RESULTS AND DISCUSSION

The optimization of dosage forms is essential in pharmaceutical development, especially for phytoconstituents, requiring a balance between therapeutic efficacy and minimized adverse effects. This process addresses challenges such as solubility, stability, topical delivery, irritation potential, and dosage optimization.

This study incorporated rose oil and oleic acid for their emollient properties, enhancing the formulation's tactile and application attributes. By combining these oils in a nanoemulsion-based gel, the formulation achieves improved stability, bioavailability, and therapeutic performance.

This innovative gel framework enables controlled drug release, reduces volatility of active constituents, and mitigates risks of rapid release, enhancing patient compliance over traditional products. The research successfully formulated and evaluated *M. pudica*-Loaded PLAROsomes nanoemugel, optimizing solubilization and minimizing side effects for effective topical delivery.

Characterization of *M. pudica*-loaded PLAROsomes nanoemugel

Physical appearance, viscosity, pH analysis, and spreadability studies

White *M. pudica*-Loaded PLAROsomes nanoemugel a viscous gel was observed. pH of formulations was found in range of 5.3–5.8. Spreadability was found to be in the range of 12.96 g cm/s.

Infrared (IR) spectrum analysis

The FTIR spectrum of the *Mimosa Pudica* extract exhibited characteristic peaks that confirm the presence of specific functional groups. A broad shape peak observed at 3353.05 cm^{-1} corresponds to O-H stretching vibration, remarking the existance of O-H funtional groups. Peaks at

2925.99 cm^{-1} and 2858.11 cm^{-1} are attributed to the asymmetric and symmetric stretching of C-H stretching bonds, respectively, suggesting aliphatic hydrocarbons. The strong absorption at 1638.27 cm^{-1} which corresponds to carbonyl (C=O) stretching, suggestive of carbonyl functional groups, while the peak at 1043.64 cm^{-1} is linked with C-O, confirming the presence of ether or ester functionalities. These results provide a comprehensive molecular fingerprint of the MIPA extract, essential for its structural characterization.

The FTIR spectrum of the MIPA-loaded PLAROsomes formulation revealed shifts and changes in peak intensities compared to the pure MIPA extract, confirming successful encapsulation and interaction with the carrier system. The O-H stretching vibration shifted from 3353.05 cm^{-1} in the extract to 3334.04 cm^{-1} in the formulation, indicating hydrogen bonding interactions. Similarly, the C-H stretching peaks at 2925.99 cm^{-1} and 2858.11 cm^{-1} in the extract shifted to 2910.14 cm^{-1} and 2841.89 cm^{-1}, respectively, suggesting changes in the hydrocarbon environment. The C=O stretching vibration exhibited a slight shift from 1638.27 cm^{-1} to 1637.12 cm^{-1}, reflecting potential interactions among the carbonyl groups of MIPA and the PLARosomal matrix. Notably, the C-O stretching peak shifted from 1043.64 cm^{-1} in the extract to 1079.28 cm^{-1} in the formulation, with a reduced peak intensity, indicating a lower concentration of free C-O groups and their involvement in the encapsulation process. These spectral changes confirm the structural integration of MIPA within the PLARosomal system.

The FTIR spectrum of the *M. pudica*-loaded PLAROsomes nanoemugel showed significant shifts and changes in peak intensities compared to the pure *M. pudica* extract, confirming successful encapsulation and interaction with the carrier system. The O-H stretching vibration, observed at 3365.23 cm^{-1} in the formulation (Fig. 1), indicated the presence of hydroxyl groups, with a shift from the extract's 3353.05 cm^{-1}, suggesting potential hydrogen bonding interactions between the extract and the PLARosomal matrix. The C-H stretching peaks at 2926.17 cm^{-1} in the formulation shifted slightly compared to those in the extract, indicating alterations in the hydrocarbon environment due to encapsulation. The C=O stretching observed at 1641.90 cm^{-1} suggests the involvement of carbonyl groups in interactions with the carrier, reflecting minor changes from the original peak position in the extract. The C-O stretching band at 1064.25 cm^{-1} exhibited a shift from the extract's peak, accompanied by a decrease in intensity, implying that the C-O groups were involved in the encapsulation process, with a reduction in their free concentration. These spectral changes confirm the successful integration of the *M. pudica* extract within the PLARosomal system.

DSC analysis

Fig. 2 represents the melting pattern of *M. pudica*-loaded PLAROsomes nanoemugel. The DSC analysis of *M. pudica*-Loaded PLAROsomes nanoemugel revealed a distinct peak at 124.16°C, with a sample weight of 9.1 mg. The corresponding area of the peak was recorded as 7583.76, and the enthalpy change (ΔH) was calculated to be 833.38 J/g. This thermal profile indicates the thermal behavior of the formulation, providing insights into its stability and the potential interactions between the *M. pudica* extract and the PLARosomal matrix.

TGA

The TGA of *M. pudica*-loaded PLAROsomes nanoemugel was performed on a sample weighing 5.683 mg. The loss on drying at 105°C was found to be 56.860% (Fig. 3), indicating the moisture content and volatile components present in the formulation. The Delta Y was also recorded as 56.860%, which corresponds to the weight loss observed during the analysis, providing information about the thermal stability and composition of the nanoemugel.

Globule size and size distribution

The *M. pudica*-loaded PLAROsomes nanoemugel exhibited a globule size of 122.9 nm, indicating a well-defined nanostructure. The Z-average was measured at 271.3, reflecting the average size distribution of the particles in the formulation. The polydispersity index value of 0.501 suggests a moderately narrow distribution, indicating that the formulation consists of relatively uniform nanoparticles with minimal size variation. These characteristics are crucial for the stability and effectiveness of the nanoemugel in drug delivery applications (Fig. 4).

Zeta potential

The zeta potential of *M. pudica*-loaded PLAROsomes nanoemugel was measured at −33.5 mV (Fig. 5), indicating good stability of the formulation due to strong electrostatic repulsion between the particles, which prevents aggregation. The electrophoretic mobility mean was recorded as −0.000259 cm^2/Vs, further confirming the stability and

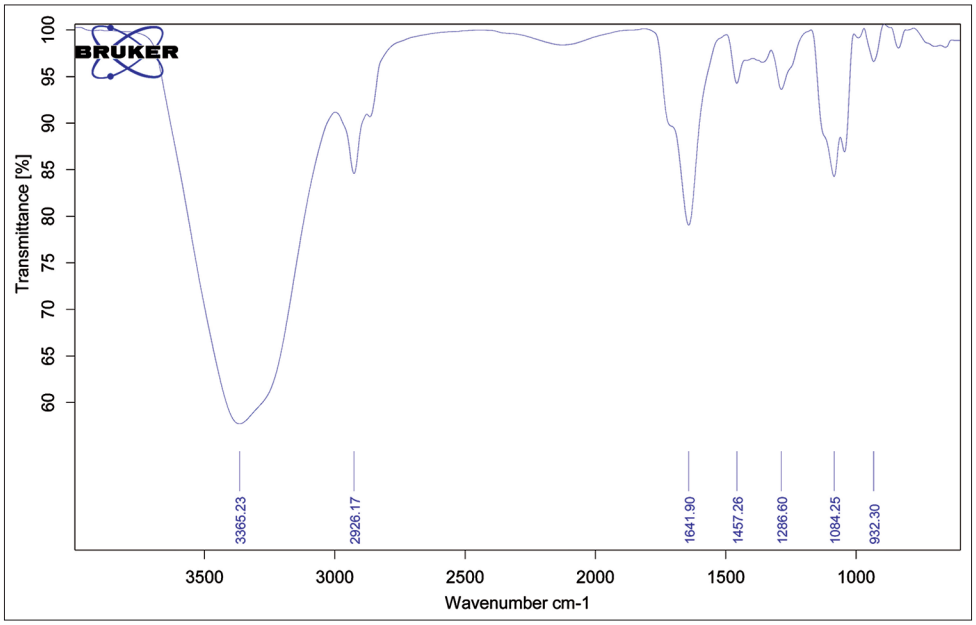

Fig. 1: Infrared spectra of *Mimosa pudica*-loaded PLAROsomes nanoemugel

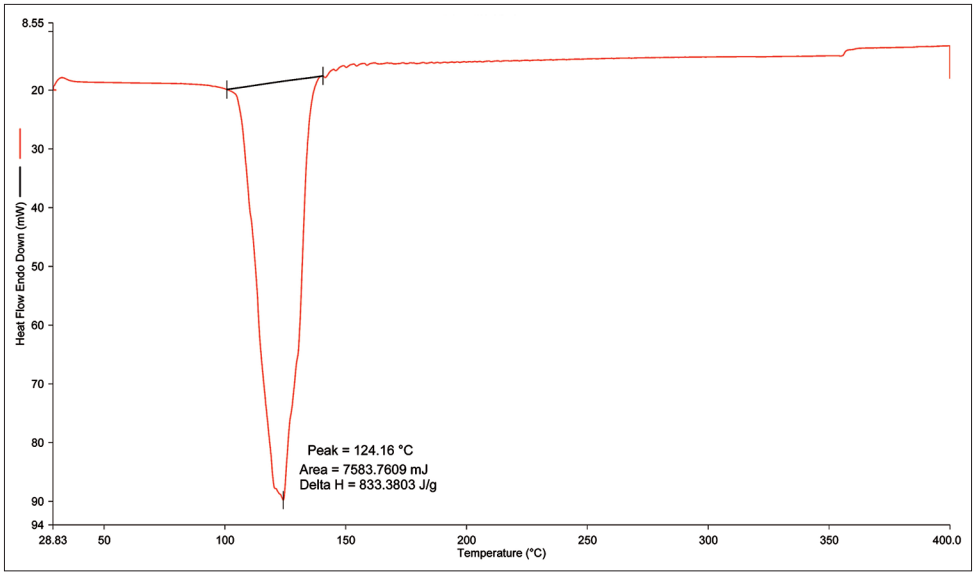

Fig. 2: Differential scanning calorimetry graph of *Mimosa pudica*-loaded PLAROsomes nanoemugel

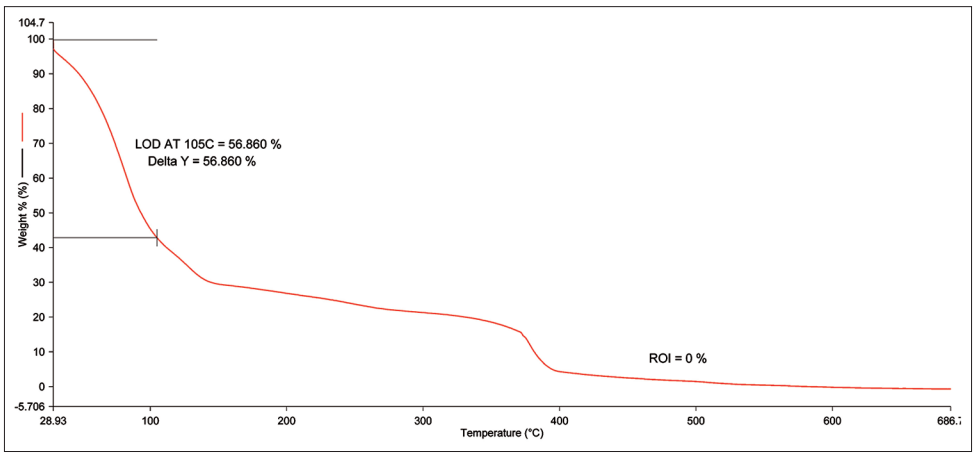

Fig. 3: Thermogravimetric analysis graph of *Mimosa pudica*-loaded PLAROsomes nanoemugel

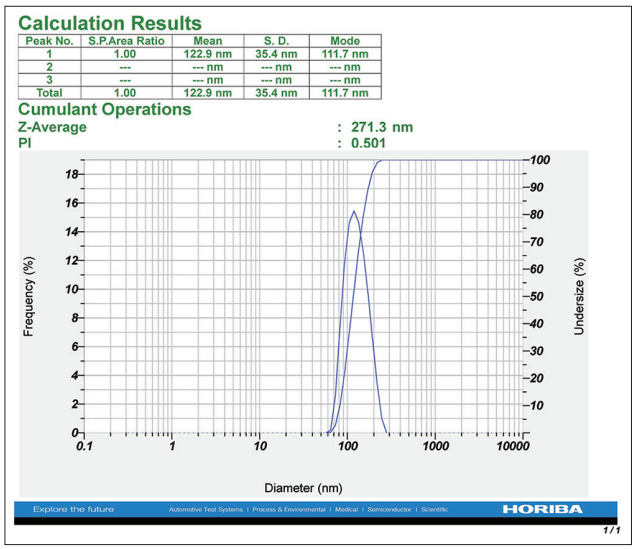

Fig. 4: Globule size analysis of *Mimosa pudica*-loaded PLAROsomes nanoemugel

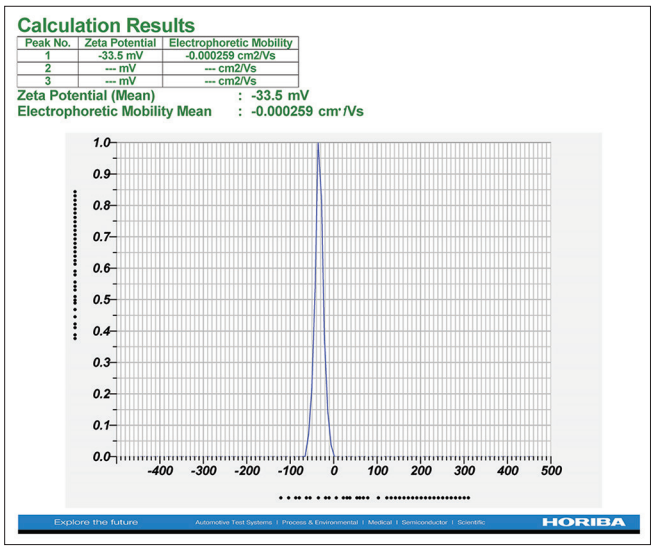

Fig. 5: Zeta potential analysis of *Mimosa pudica*-loaded PLAROsomes nanoemugel

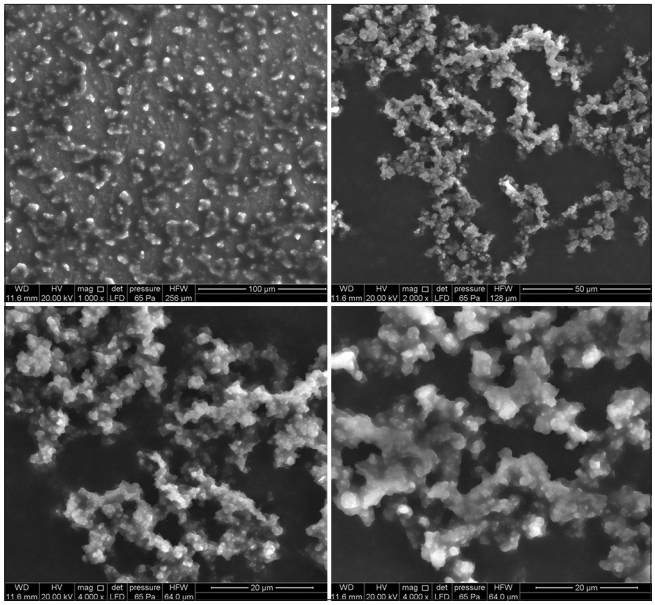

Fig. 6: Scanning electron microscopy analysis of *Mimosa pudica*-loaded PLAROsomes nanoemugel

surface charge characteristics of the formulation. These findings suggest that the nanoemugel has a stable colloidal dispersion, which is essential for consistent drug release and enhanced therapeutic performance.

Scanning electron microscopy (SEM)

The SEM analysis of *M. pudica*-loaded PLAROsomes nanoemugel revealed agglomeration of the particles, with circular shapes observed at various magnifications. This agglomeration may indicate particle clustering, which is typical in nanoscale formulations. The circular morphology suggests uniformity in the nanoparticle structure, though further optimization may be needed to minimize aggregation and improve the overall stability and performance of the formulation.

TEM

The TEM analysis of *M. pudica*-Loaded PLAROsomes Nanoemugel revealed particles with a circular shape, indicating a well-defined structure at the nanoscale. The average particle size was found to be 82.3±12 nm (Fig. 7), demonstrating that the formulation consists of relatively uniform nanoparticles. This size range is consistent with the desired characteristics for effective drug delivery and stability in therapeutic applications.

In vitro drug release

The drug release profile of *M. pudica*-loaded PLAROsomes nanoemugel was estimated over a 48-h period, and the cumulative release percentage was recorded at various time intervals. After 1 h, the release reached 6.25%, which steadily increased to 14.23% at 2 h and 29.35% at 4 h. By 8 h, the release percentage rose to 38.98%, further progressing to 50.21% at 16 h. A significant release of 59.85% was observed at 32 h, and the maximum cumulative release recorded was 68.25% at the 48-h mark (Fig. 8a), indicating a sustained release pattern characteristic of PLAROsomes.

The release kinetics of the *M. pudica*-loaded PLAROsomes nanoemugel were evaluated using various mathematical models to determine the best-fit release mechanism [41-43]. The Korsmeyer–Peppas model exhibited the highest correlation coefficient (R^2=0.9931), indicating that the drug release follows a non-Fickian diffusion mechanism, suggesting both diffusion and polymer relaxation contribute to the release. The Higuchi model also showed a strong correlation (R^2=0.9497), supporting the involvement of diffusion as a key release mechanism. The first-order model (R^2=0.9037) indicated a concentration-dependent

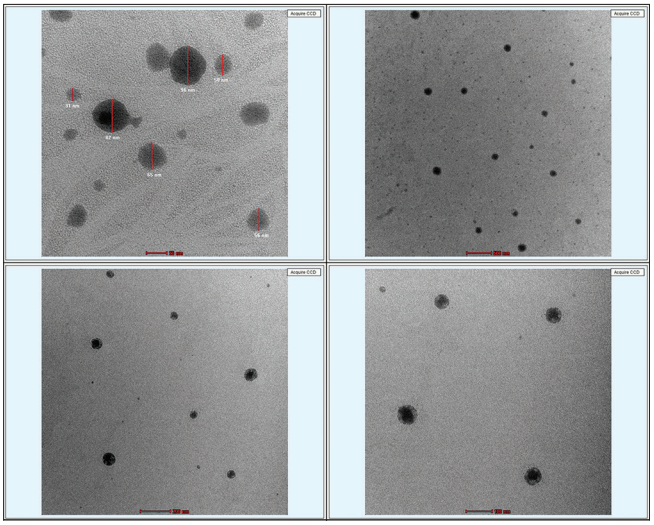

Fig. 7: Transmission electron microscopy analysis of *Mimosa pudica*-loaded PLAROsomes nanoemugel

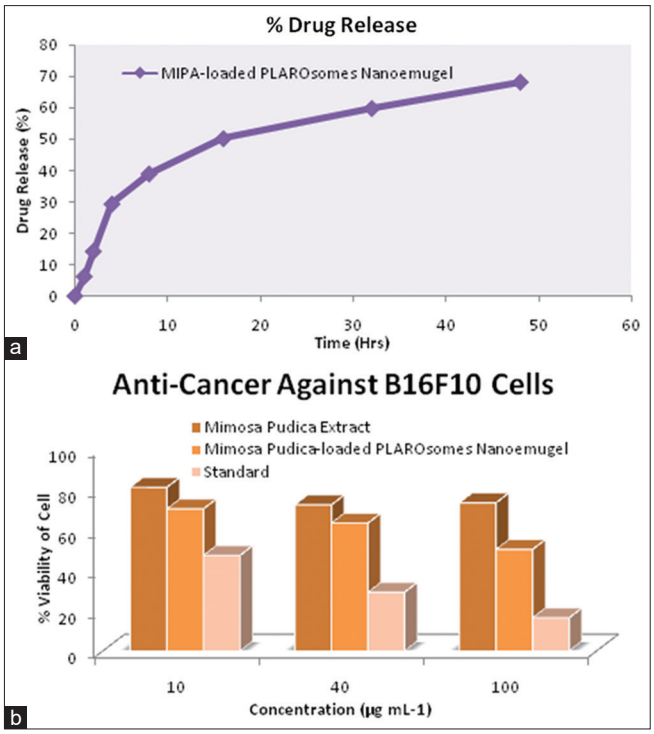

Fig. 8: % Drug release (a) Anti-cancer activity (b) of *Mimosa pudica*-loaded PLAROsomes nanoemugel

release, while the Hixson–Crowell model (R^2=0.8708) suggested some influence of formulation geometry on drug release. The zero-order model showed the lowest fit (R^2=0.797), indicating that the release is not entirely independent of concentration. These findings confirm that the Korsmeyer–Peppas model is the most appropriate for describing the drug release behavior of the formulation.

Stability studies

The *M. pudica*-loaded PLAROsomes nanoemugel exhibited remarkable stability when stored at 25°C and 30°C for 1, 3, and 6 months. At 40°C, the formulation maintained stability for up to 3 months, with no significant alterations in % drug content or pH. However, after 6 months at this temperature, considerable changes were observed in globule size, zeta potential, and viscosity, indicating reduced stability under these conditions. These findings suggest that the formulation is

Table 2: % of viability the *M. pudica*-loaded PLAROsomes nanoemugel treated cell lines by MTT assay

Concentration (μg mL^{-1})	B16F10 (Mouse skin melonoma cell line)		
	***M. pudica* extract**	***M. pudica*-loaded PLAROsomes nanoemugel**	**Standard (5-FU)**
10	80.90±1.2325^{ns}	70.25±1.2547*	47.25±1.3567
40	72.25±0.2547^{ns}	63.25±1.0245*	29.01±0.8971
100	73.25±0.9871*	50.21±1.5467*	16.40±1.2450

Statistical significance levels were denoted as follows: ns: Not significant, p<0.05 (*), p<0.01 (**) and p<0.001 (***). *M. pudica*: *Mimosa pudica*

well-suited for long-term storage at moderate temperatures, though it is less stable when exposed to elevated temperatures over extended durations.

***In vitro* cytotoxicity assay**

The anticancer activity of *M. pudica* extract, *M. pudica*-loaded PLAROsomes nanoemugel, and the standard was evaluated against B16F10 melanoma cells at concentrations of 10, 40, and 100 μg mL^{-1}. MIPA exhibited cell viability percentages of 80.9%, 72.25%, and 73.25% (Fig. 8b and Table 2), respectively, across the tested concentrations. In contrast, the MIPA-loaded PLAROsomes nanoemugel demonstrated enhanced efficacy with cell viability percentages of 70.25%, 63.25%, and 50.21%, suggesting improved cytotoxic effects due to the nanocarrier system. The standard showed the most potent activity, with cell viability percentages of 47.25%, 29.01%, and 16.4%, indicating its strong inhibitory effect [44,45]. These results highlight the potential of the MIPA-loaded PLAROsomes nanoemugel as an effective anticancer formulation, particularly in comparison to the free extract.

CONCLUSION

The *M. pudica*-loaded PLARosome-based nanoemugel was successfully formulated using a novel combination of Carbopol Ultrez 10, oleic acid, and rose oil. The formulation was thoroughly characterized using various techniques, including IR, DSC, TGA, zeta potential, particle size analysis, SEM, and TEM. TEM analysis confirmed the presence of well-defined globules with uniform size, indicative of a stable and efficient nanoemugel system. *In vitro* cytotoxicity studies against B16F10 melanoma cells demonstrated significant anticancer activity, highlighting the potential of the developed formulation as a promising therapeutic candidate for melanoma treatment. Future perspectives include conducting *in vivo* studies to evaluate the pharmacokinetic profile and therapeutic efficacy, as well as exploring the formulation's potential in targeting other cancer types and advancing its clinical application.

AUTHOR'S CONTRIBUTIONS

Vaishali Gaikwad: Investigation, conceptualization, drafting, supervision. Ravindra Laware: Review, editing, and visualization. Nitin Mohire: Writing review and editing. Somnath Bhinge: Writing and analysis.

CONFLICTS OF INTEREST

Authors do not have any conflict of interest.

FUNDING

None.

REFERENCES

1. Rieger MM. Barrier function of the skin. J Soc Cosmet Chem. 2001;42:129-34.
2. Siegel RL, Miller KD, Jemal A. Cancer statistics, 2020. CA Cancer J Clin. 2020;70(1):7-30. doi: 10.3322/caac.21590, PMID 31912902
3. Armstrong BK, Kricker A. How much melanoma is caused by sun exposure? Melanoma Res. 1993;3(6):395-401. doi: 10.1097/00008390-199311000-00002, PMID 8161879
4. Urbach F. Incidence of nonmelanoma skin cancer. Dermatol Clin. 1991;9(4):751-5.
5. Leiter U, Garbe C. Epidemiology of melanoma and nonmelanoma skin cancer--the role of sunlight. Adv Exp Med Biol. 2008;624:89-103. doi: 10.1007/978-0-387-77574-6_8, PMID 18348450
6. Benson HA. Transdermal drug delivery: Penetration enhancement techniques. Curr Drug Deliv. 2005;2(1):23-33. doi: 10.2174/1567201052772915, PMID 16305405
7. Prausnitz MR, Langer R. Transdermal drug delivery. Nat Biotechnol. 2008;26(11):1261-8. doi: 10.1038/nbt.1504, PMID 18997767
8. Müller RH, Petersen RD, Hommoss A, Pardeike J. Nanostructured lipid carriers (NLC) in cosmetic dermal products. Adv Drug Deliv Rev. 2007;59(6):522-30. doi: 10.1016/j.addr.2007.04.012
9. Shakeel F, Shafiq S, Haq N, Alanazi FK, Alsarra IA. Nanoemulsions as potential vehicles for transdermal and dermal delivery of hydrophobic compounds. Drug Dev Ind Pharm. 2010;36(11):1251-62.
10. Preeti, Sambhakar S, Malik R, Bhatia S, Al Harrasi A, Rani C, et al. Nanoemulsion: An emerging novel technology for improving the bioavailability of drugs. Scientifica (Cairo). 2023;2023:6640103. doi: 10.1155/2023/6640103
11. Hashem FM, Shaker DS, Ghorab MK, Nasr M, Ismail A. Formulation, characterization, and clinical evaluation of microemulsion containing clotrimazole for topical delivery. AAPS PharmSciTech. 2011 Sep;12(3):879-86. doi: 10.1208/s12249-011-9653-7
12. Nadkarni KM. Indian Materia Medica. Mumbai: Bombay Popular Prakashan; 2009.
13. Patel SS, Jesuraj SA, Kumar ES, Saminathan K, Suthakaran R, Kumar MR, *et al*. Wound healing activity of *Mimosa pudica* Linn formulation. Asian Pac J Trop Biomed. 2012;2(6):543-7.
14. Vallinayaki KN, Shanmugam R. Evaluation of antidiabetic activity and cytotoxic effect of strontium nanoparticles synthesized using Mimosa pudica. J Pharm Bioallied Sci. 2024;16 Suppl 2:S1340-S4. doi: 10.4103/jpbs jpbs_583_23
15. Batra P, Sharma AK. Anti-cancer potential of flavonoids: Recent trends and future perspectives. 3 Biotech. 2013;3(6):439-59. doi: 10.1007/s13205-013-0117-5
16. Rice-Evans C, Miller N, Paganga G. The antioxidant properties of flavonoids and phenolic acids. Trends Plant Sci. 1997;2(4):152-9. doi: 10.1016/S1360-1385(97)01018-2
17. Pandey KB, Rizvi SI. Plant polyphenols as dietary antioxidants in human health and disease. Oxid Med Cell Longev. 2009;2(5):270-8. doi: 10.4161/oxim.2.5.9498
18. Jin C, Wang K, Oppong-Gyebi A, Hu J. Application of nanotechnology in cancer diagnosis and therapy - a mini-review. Int J Med Sci. 2020;17(18):2964-73. doi: 10.7150/ijms.49801
19. Tayeb HH, Felimban R, Almaghrabi S, Hasaballah N. Nanoemulsions: Formulation, characterization, biological fate, and potential role against COVID-19 and other viral outbreaks. Colloid Interface Sci Commun. 2021;45:100533. doi: 10.1016/j.colcom.2021
20. Jin C, Wang K, Oppong-Gyebi A, Hu J. Application of nanotechnology in cancer diagnosis and therapy - a mini-review. Int J Med Sci. 2020;17(18):2964-73. doi: 10.7150/ijms.49801
21. Kangara D, Maanisha NW, De Silva HH, Wickramaratne M. Formulation and Development of Mimosa Pudica and Glycyrrhiza Glabra Containing Topical Cream for Hyperpigmentation. In: Bachelor's Thesis, Industrial Pharmaceutical Science; 2024 Jul. doi: 10.13140/RG.2.2.11046.54087
22. Kumar VR, Kumar S. Formulation and evaluation of Mimosa pudica gel. Int J Pharm Pharm Sci. 2011;3(1):55-7.
23. Patil PS, Salunkhe VR, Bhinge SD, Patil SB, Kumbhar BV. Formulation optimization and evaluation of glycyrrhetinic acid loaded PLARosome using factorial design: *In-vitro* anti-ulcer activity and in silico PASS prediction. J Indian Chem Soc. 2021;98(11):100199. doi: 10.1016/j.jics.2021.100199
24. Moghimipour E, Salami A, Monjezi M. Formulation and evaluation of liposomes for transdermal delivery of celecoxib. Jundishapur J Nat Pharm Prod. 2015;10(1):e17653. doi: 10.17795/jjnpp-17653, PMID 27747190
25. Gaikwad VK, Laware RB, Mohire NC, Bhinge SD. PLAROsomes as a modified liposomes delivery system for *Mimosa pudica* L. extract: Augmenting anticancer potential against prostate and skin cancer cell lines. Ann Pharm Fr. 2025:S0003-4509(25)00074-4. doi: 10.1016/j.pharma.2025.04.004.
26. Akbarzadeh A, Rezaei-Sadabady R, Davaran S, Joo SW,

Zarghami N, Hanifehpour Y, *et al*. Liposome: Classification, preparation, and applications. Nanoscale Res Lett. 2013;8(1):102. doi: 10.1186/1556-276X-8-102, PMID 23432972

27. Jadhav ST, Salunkhe VR, Bhinge SD. Nanoemulsion drug delivery system loaded with imiquimod: A QbD-based strategy for augmenting anti-cancer effects. Future J Pharm Sci. 2023;9(1):120. doi: 10.1186/s43094-023-00568-z
28. Jadhav ST, Salunkhe VR, Bhinge SD, Honmane SM, Jadhav AS. Development and evaluation of imiquimod-loaded nanoemulsion-based gel for the treatment of skin cancer. Future J Pharm Sci. 2024;10(1):93. doi: 10.1186/s43094-024-00660-y
29. Kumar L, Verma R. *In vitro* evaluation of topical gel prepared using natural polymer. Int J Drug Delivery. 2010;2(1):58-63. doi: 10.5138/ijdd.2010.0975.0215.02012
30. Gaber DA, Alsubaiyel AM, Alabdulrahim AK, Alharbi HZ, Aldubaikhy RM, Alharbi RS, *et al*. Nano-emulsion based gel for topical delivery of an anti-inflammatory drug: *In vitro* and *in vivo* evaluation. Drug Des Dev Ther. 2023;17:1435-51. doi: 10.2147/DDDT.S407475, PMID 37216175
31. Shi Y, Zhang M, Chen K, Wang M. Nano-emulsion prepared by high pressure homogenization method as a good carrier for Sichuan pepper essential oil: Preparation, stability, and bioactivity. LWT. 2022;154:112779. doi: 10.1016/j.lwt.2021.112779
32. Bhinge SD, Kamalakar SP, Randive DS, Bhutkar MA, Patil KS, Merekar AN, *et al*. Development and characterization of stable proanthocyanidin-loaded PLAROsomes as a potential drug carrier system for augmenting anticancer activity. Eur J Lipid Sci Technol. 2024;126(6):2300218. doi: 10.1002/ejlt.202300218
33. Lu WC, Huang DW, Wang CR, Yeh CH, Tsai JC, Huang YT, *et al*. Preparation, characterization, and antimicrobial activity of nanoemulsions incorporating citral essential oil. J Food Drug Anal. 2018;26(1):82-9. doi: 10.1016/j.jfda.2016.12.018, PMID 29389592
34. Gibis M, Ruedt C, Weiss J. *In vitro* release of grape-seed polyphenols encapsulated from uncoated and chitosan-coated liposomes. Food Res Int. 2016;88(A):105-13. doi: 10.1016/j.foodres.2016.02.010, PMID 28847389
35. Patil SS, Chougale RD, Manjappa AS, Disouza JI, Hajare AA, Patil KS. Statistically developed docetaxel-laden mixed micelles for improved therapy of breast cancer. OpenNano. 2023;9:100079. doi: 10.1016/J.ONANO.2022.100079
36. Wallace SJ, Li J, Nation RL, Boyd BJ. Drug release from nanomedicines: Selection of appropriate encapsulation and release methodology. Drug Deliv Transl Res. 2012;2(4):284-92. doi: 10.1007/s13346-012-0064-4, PMID 23110256
37. Bagal AV, Vijay N, Disouza J, Mali GU, Bhinge SD. Anticancer potential of Hemidesmus indicus-enriched Pt/Au bimetallic nanoparticles against human breast and skin cancer cell lines. Nanosci Nanotechnol Asia. 2023;13(6):e281123223950. doi: 10.2174/012210681226654223111707 3659
38. Bhutkar MA, Randive DS, Bhinge SD, Wadkar GH, Todkar SS, Shejawal KP. Development of gold, silver and iron nanoparticles of isolated berberine: its characterization, antimicrobial, and cytotoxic activities against COLO320DM and HeLa cells. Gold Bull. 2022;55(1):93-103. doi: 10.1007/s13404-022-00309-9
39. Shejawal KP, Randive DS, Bhinge SD, Bhutkar MA, Wadkar GH, Todkar SS, *et al*. Functionalized single-walled carbon nanotube for colon targeted delivery of isolated lycopene from Lycopersicon esculentum in colorectal cancer: Its *in-vitro* cytotoxicity and *in-vivo* roentgenographic study. J Mater Res. 2021;36(24):4894-907. doi: 10.1557/s43578-021-00431-y
40. Bhat SS, Revankar VK, Kumbar V, Bhat K, Kawade VA. Synthesis, crystal structure and biological properties of a cis-dichloridebis (diimine)copper(II) complex. Acta Crystallogr Sect C Struct Chem. 2018;C74:146-51.
41. Bhinge SD, Jadhav S, Lade P, Bhutkar MA, Gurav S, Jadhav N, *et al*. Biogenic nanotransferosomal vesicular system of *Clerodendrum serratum* L. for skin cancer therapy: Formulation, characterization, and efficacy evaluation. Future J Pharm Sci. 2025;11(1):5. doi: 10.1186/s43094-024-00755-6.
42. Bhinge SD, Kamalakar SP, Randive DS, Bhutkar MA, Patil KS, Merekar AN, *et al.* Development and characterization of stable proanthocyanidin-loaded PLAROsomes as a potential drug carrier system for augmenting anticancer activity. Eur J Lipid Sci Technol. 2024;126(6):2300218. doi: 10.1002/ejlt.202300218
43. Bhinge SD, Kamalakar SP, Randive DS, Bhutkar MA, Patil KS, Merekar AN, *et al*. Development and characterization of stable proanthocyanidin-loaded PLAROsomes as a potential drug carrier system for augmenting anticancer activity. Eur J Lipid Sci Technol. 2024;126(6):2300218. doi: 10.1002/ejlt.202300218
44. Bhinge SD, Kamble S, Randive D, Bhutkar M, Nadaf S, Merekar A, *et al*. Development, characterization, and assessment of PLAROsomal vesicular system of curcumin for enhanced stability and therapeutic efficacy. Future J Pharm Sci. 2024;10(1):161. doi: 10.1186/s43094-024-00733-y
45. Gauru I, Alam YS, Santoso M, Fadlan A, Affifah NR, Andifa N, *et al*. *In silico* studies and cytotoxicity assay of benzylidene benzo hydrazide derivatives on cancer stem cell. Int J Appl Pharm. 2025;17:134-41. doi: 10.22159/ijap.2025v17i2.53105
46. Jose M, Jaison AC, Mathew A, Suku A, Venugopal S, Jayalakshmi PM. *In-vitro* cytotoxic study on root extracts of *Apama siliquosa* Lamk. Int J Pharm Sci Res. 2021;23:3805-13.